

New anti-fluorite solid-solution phases in Li–Ti–N ternary system

Atsuo YAMADA, Shunsuke MORI, Hiromasa IYAMA, Ryoji KANNO and Masatoshi SHIBATA*

Department of Electronic Chemistry, Interdisciplinary Graduate School of Science and Engineering,
Tokyo Institute of Technology, 4259, Nagatsuta, Midori-ku, Yokohama 226-8502

*Functional Materials Laboratory, Central Research Laboratories, Idemitsu Kosan Co., Ltd.,
1280, Kami-Izumi, Sodegaura, Chiba 299-0293

New Li–Ti–N solid-solution compounds with an anti-fluorite-type superstructure were synthesized by heating the mixture of Li₃N and TiN at 800°C in Ar flow. The compositions of the new compounds seem to lie on the tie-line between the two well-known compounds, Li₃N (hexagonal, *P*6/*mmm*) and Li₅TiN₃ (cubic, *I*2₁/*a*-3) by Li evaporation during heating in Ar gas flow, and nominally represented with Li_{5+y}Ti_{1-y}N_{3-y}. The solubility is large; the anti-fluorite-type superstructure of Li₅TiN₃ (*y* = 0) was retained up to *y* = ca. 0.9, which is close to the end member Li₃N (*y* = 1) with a different layered structure. This finding opens up further exploring other new Li–M–N (*M* = transition metals, group XIII, or XIV elements) phases with some attractive functions.

©2009 The Ceramic Society of Japan. All rights reserved.

Key-words : Anti-fluorite, Lithium nitride, Titanium

[Received August 25, 2008; Accepted November 20, 2008]

1. Introduction

Lithium nitride and lithium metal nitrides form a promising materials group for energy storage and conversions, such as anode for lithium secondary battery, lithium ion conductor, and hydrogen storage. For example, Li₇MnN₄ (200 mAh/g, 1.2 V vs. Li/Li⁺),¹⁾ Li₃FeN₂ (130 mAh/g, 1.2 V vs. Li/Li⁺),²⁾ Li_{2.7}Fe_{0.3}N (550 mAh/g, 0.05–1.3 V vs. Li/Li⁺),³⁾ Li_{2.6}Co_{0.4}N (700–900 mAh/g, 0.6 V vs. Li/Li⁺),⁴⁾ Li_{2.5}Ni_{0.5}N (400 mAh/g, 0.6 V vs. Li/Li⁺),⁴⁾ and Li_{2.5}Cu_{0.5}N (400 mAh/g, 0.6 V vs. Li/Li⁺)⁴⁾ were reported to show reversible lithium deintercalation and reintercalation. In particular, Li_{2.6}Co_{0.4}N has attracted much attention of battery engineers because of its large reversible capacity with a function of lithium source. As lithium ion conductors, Li₃N itself shows high lithium conductivity of > 10⁻³ Scm⁻¹ at room temperature but its low decomposition voltage of 0.44 V vs. lithium has prohibited to be used for practical application.⁵⁾ To combat this problem, ternary systems such as Li_{3-x}Cu_xN₃,^{6,7)} Li₃BN₂,^{8,9)} Li₃AlN₂,^{10,11)} and Li–Si–N^{12,13)} phases were thoroughly investigated. Recently, Chen et al.¹⁴⁾ reported a large hydrogen storage capacity of 6.7 wt% upon Li₃N under 0.3 MPa of H₂ at 255–285°C by reversible decomposition into lithium amide, LiNH₂, or lithium imide, Li₂NH.

As for Li–M–N ternary system, where *M* = 3*d* transition metals, the general acceptance is that the anti-fluorite (anti-CaF₂) structure with general chemical formula, Li_{2*n*-1}*MN_n*, is stabilized when *M* is early transition metals, Sc–Fe, as Li₅TiN₃ (*n* = 3),¹⁵⁾ Li₇VN₄ (*n* = 4),¹⁶⁾ Li₁₅Cr₂N₉ (*n* = 4.5),¹⁷⁾ Li₆CrN₄ (*n* = 4),¹⁷⁾ Li₇MnN₄ (*n* = 4),¹⁸⁾ and Li₃FeN₂ (*n* = 2),¹⁹⁾ where nitrogen atoms form cubic closed packed sub-array (Ca site in fluorite CaF₂) and all of the tetrahedral sites (F sites in fluorite CaF₂) are occupied by lithium or transition metal atoms with regular arrangements. While, Li₃N-type structure is the ground state forming solid solutions as Li_{3-y}*M_y*N when *M* is late transition metals, Co, Ni, and Cu.^{20,21)} Lithium nitride has a layered structure belonging to the space group *P*6/*mmm* with two different lithium sites, Li(1) and Li(2). The Li₂N layer is formed by Li(2) in ab plain with edge-shared NLi₆ hexa-

gons and Li(1) positions between layers to form continuous Li(1)–N–Li(1) chain along *c*-axis. Although such an overall classification shown in Fig. 1 has been well established, detailed phase relationship depending on the synthetic conditions and/or Li/M ratio has to our knowledge not been documented before.

In this paper, we took a closer look at the Li–Ti–N ternary system towards some new phases which may not be categorized into the above empirical general rule. Attention was focused on the effect of Li/Ti ratio in the starting precursor as well as of the atmospheric gas in the sintering processes. In the previous literature, anti-fluorite-type Li₅TiN₃ has been believed to be the only stable phase in the Li–Ti–N ternary system and synthesized by sintering Li₃N and TiN at 1040–1080°C under NH₃ or N₂ gas. The external nitrogen source is necessary because the line between Li₃N and TiN positions in the nitrogen-poor region in the ternary phase diagram as compared with the Li₅TiN₃ point (Fig. 2). Our principal concern at this stage was that some new phases may be obtained by sintering under inert atmosphere without nitrogen.

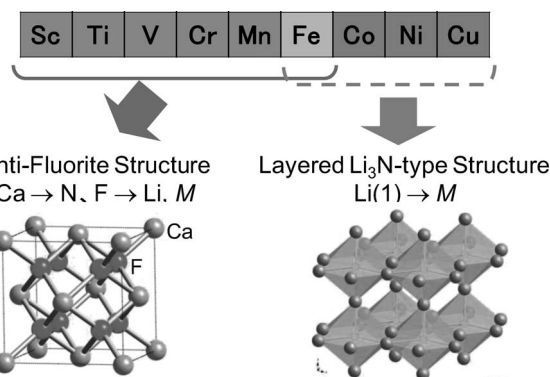


Fig. 1. Overall structural classification of Li–M–N ternary compounds, where *M* is the 3*d* transition metals.

2. Experiments

Powders were synthesized via a solid-state reaction. All procedure, including sample transport, mixing, sintering, was performed in an inert atmosphere (dewpoint < -65°C). Lithium nitride Li₃N (High Purity Chemical Co., > 99.99%) and titanium nitride TiN (Wako Pure Chemical Ind., Ltd., > 98.7%) were used as starting materials; the molar ratio x in $x\text{Li}_3\text{N}:(100-x)\text{TiN}$ was varied from 65 to 97.5, as indicated in Fig. 2. A total of approximately 4 g were sealed into a 250-ml Cr-hardened SUS container together with a mixture of 10 mmφ × 5 and 5 mmφ × 30 Cr-hardened SUS balls. This was thoroughly mixed and reground by conventional planetary milling (Ito Co., LP-4) for 6 h at 240 rpm, followed by sintering at 700–800°C for 24 h in a pellet form under a Ar (99.9995%) or N₂ (99.9999%) gas flow with 50 cc/min. Heating and cooling rate was 8°C/min. Sintering was performed using molybdenum sample boat set in the SUS reactor tube.

X-ray diffraction patterns of the powdered samples were obtained with an X-ray diffractometer (Rigaku Co. RAD-C, 12 kW) with Cu K α radiation. The diffraction data were collected at 0.02 step widths over a 2θ range from 10° to 100°. The chemical compositions of the final products were checked by atomic absorption spectrometer (Hitachi, Ltd., Z-2300).

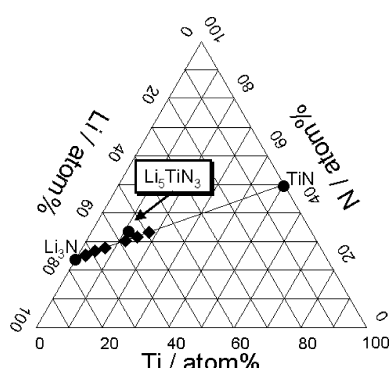


Fig. 2. Li-Ti-N ternary diagram.

X-ray absorption spectroscopy for Ti K-edge was performed using LOOPER 2000 (Rigaku Co.) with an energy step in 1 eV. The sample was firmly sealed into KAPTON film to avoid any contamination by reacting with air and/or moisture. Standard samples of TiO (Aldrich, 99.9%) and rutile TiO₂ (High Purity Chemicals Co., Ltd., 99.9%) were used.

3. Results and discussions

Powder X-ray diffraction profiles measured for samples obtained by sintering the mixture of various Li₃N:TiN molar ratios at 800°C are given in Fig. 3. Details on the identified phases are summarized in Fig. 4. Even at a first glance, the phases sintered under N₂ and Ar were entirely different. The color of samples prepared under N₂ was always dark brown or dark grey, while the color of samples prepared under Ar was always pale yellow.

The dark color is the signal of residual starting materials, Li₃N (dark reddish brown) or TiN (dark blue-green). This is also supported by the X-ray diffraction profiles themselves, where the samples sintered under N₂ was complicated and analyzed as a mixture of anti-fluorite derivatives, low-temperature stable phase Li₈TiN₄,²² Li₃N-related phase, and residual TiN. Apparently, the reaction in N₂ gas is incomplete at 800°C and is consistent with the previous report that much higher temperature of > 1000°C is necessary to synthesize the single phase of Li₅TiN₃ with an anti-fluorite-type superstructure even under NH₃ atmosphere.¹⁵

On the other hand, the samples synthesized in the Ar flow showed a systematic change of X-ray diffraction (XRD) profile maintaining the anti-fluorite-type structure framework. For a wide range of starting molar ratio between $x = 65$ and $x = 95$, no parasite signal was observed and all diffraction peaks were indexed with a cubic lattice of the anti-fluorite-type structure framework. The major systematic changes as a function of x were found in the suppression in (211), (312) peaks, the simultaneous enhancement in (222) peak, and the monotonic decrease in the cubic lattice constant as shown in Fig. 5. Note that the lattice constant for the sample with starting molar ratio $x = 65$ is close to that of the well-known anti-fluorite-type Li₅TiN₃. It is also noteworthy that the anti-fluorite-type structure framework is

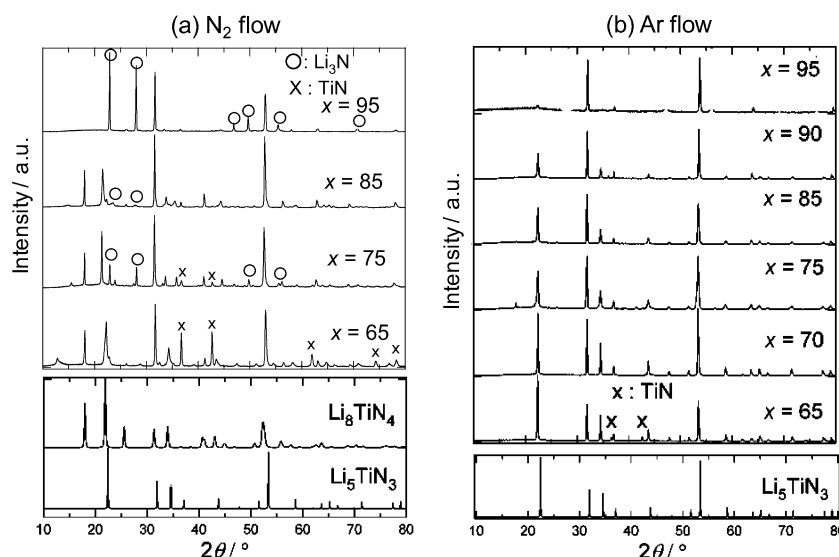


Fig. 3. XRD patterns of the compounds obtained by sintering $x\text{Li}_3\text{N}-(100-x)\text{TiN}$ mixture at 800°C under N₂ flow (a) and under Ar flow (b).

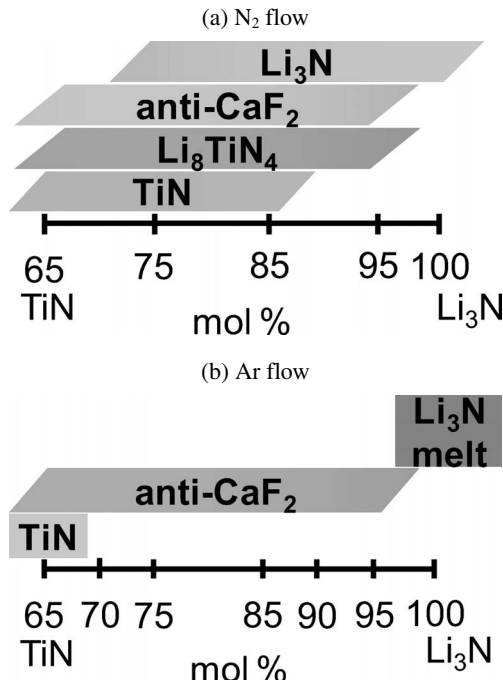


Fig. 4. Schematic derivation of the final products by sintering TiN/Li₃N mixture in various ratios at 800°C under (a) N₂ flow and (b) Ar flow.

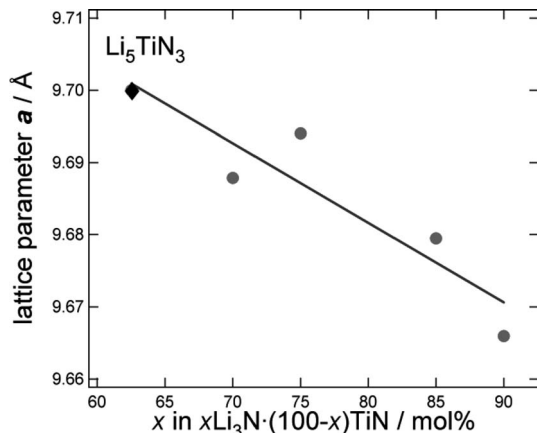


Fig. 5. Variation of the lattice constant for the new anti-fluorite phase obtained by sintering $x\text{Li}_3\text{N} \cdot (100-x)\text{TiN}$ mixtures at 800°C in Ar flow.

retained up to $x = 95$, which is close to the end member Li₃N($x = 100$) with entirely a different layered structure.

Based on the preceding results, overall schematic diagram for final products along TiN-Li₃N binary line ($65 < x < 100$) are given in Fig. 4. The emphasis is given to the differences when they are sintered in N₂ and Ar flow. Three major differences are i) for almost whole region of $65 < x < 100$, continuous solid solution forms in Ar, whereas multi-phase mixture is always the case in N₂, ii) the presence of residual starting materials, Li₃N and TiN, in N₂ by incomplete reaction, and iii) the presence of Li₈TiN₄ phase in N₂. The existence of Li₈TiN₄ phase (*P4₂/hmc*) has just recently been reported²²⁾ and it can be synthesized only by the low-temperature (< 400°C) sintering in N₂ flow. Therefore, it is reasonable that any Li₈TiN₄ phase was not found in the sample sintered at relatively high temperature of 800°C in Ar flow.

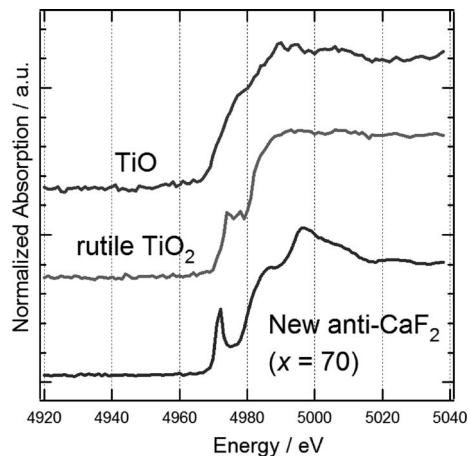


Fig. 6. Ti K-edge X-ray absorption near edge spectra of the new compound with anti-fluorite structure obtained by sintering the $x\text{Li}_3\text{N} \cdot (100-x)\text{TiN}$ mixture ($x = 70$) in Ar flow.

Hereafter, we will focus on the new continuous solid solutions obtained by sintering at 800°C in Ar (Figs. 3(b) and 4(b)). First of all, X-ray absorption spectra of Ti K-edge measured for the sample from Li₃N:TiN = 75:25 mixture is shown in Fig. 6, together with those of standard samples, TiO and rutile TiO₂. It is reasonable that the absorption edge is at much higher energy than that of Ti²⁺O and rather close to that of Ti⁴⁺O₂, as the color of the whole series of samples was pale yellow, which is as same as that of Li₅Ti⁴⁺N₃. Note that the immediate electrochromic response to dark blue is general when there is even a slight reduction of Ti from tetravalent. The pre-edge feature A is due to the dipole forbidden 1 s 3d transition, which has been known to become visible under the lower symmetry with significant shift in the peak position to lower energy.^{23),24)} Indeed, negligible pre-edge feature was observed for Ti in the symmetric octahedral sites in TiO, while the pre-edge structure is clear for rutile TiO₂ where the TiO₆ octahedra are strongly distorted. In the present new Li-Ti-N sample, the pre-edge peak is much more pronounced with a clear shift to the lower energy, and hence it is reasonable to speculate that Ti is located in the tetrahedral 16c site in the original anti-fluorite structure. Contribution from the Ti migrated to the vacant octahedral 24d site is unlikely because of its highly symmetric environment.

Following these tracks, here we show the results of profile simulations by assuming that all Ti atoms are fixed in the tetrahedral 16c sites and are always tetravalent. Two possible structural models were considered; (a) titanium are substituted by the excess lithium y with simultaneous formation of the nitrogen defect y for charge neutrality, thereby the solid solution can be written as [Li₅]₄₈[Li_yTi_{1-y}]_{16c}[N_{3-y}]_{8a,24d}, and (b) the excess lithium occupy not only the original Ti 16c sites but also the vacant octahedral 24d sites, thereby the solid solution can be written as [Li₅]₄₈[Li_{3y}]_{24d}[Li_yTi_{1-y}]_{16c}[N₃]_{8a,24d}. Figure 7 summarizes the simulation results, which obviously show the model (a) gives more reasonable profiles close to the experimental results. Loss of lithium during the synthesis was estimated to be ca. 3 percent of the total lithium by atomic absorption spectroscopy, which might be responsible to adjust the final composition into the Li₃N-Li₅TiN₃ (Li_{5+y}Ti_{1-y}N_{3-y}) tie-line maintaining Ti in tetravalent state, as the Li₃N-TiN raw materials line (Ti in trivalent state) positions slightly lithium-rich side of the final product (see Fig. 2). Although it is likely that nitrogen defects function for

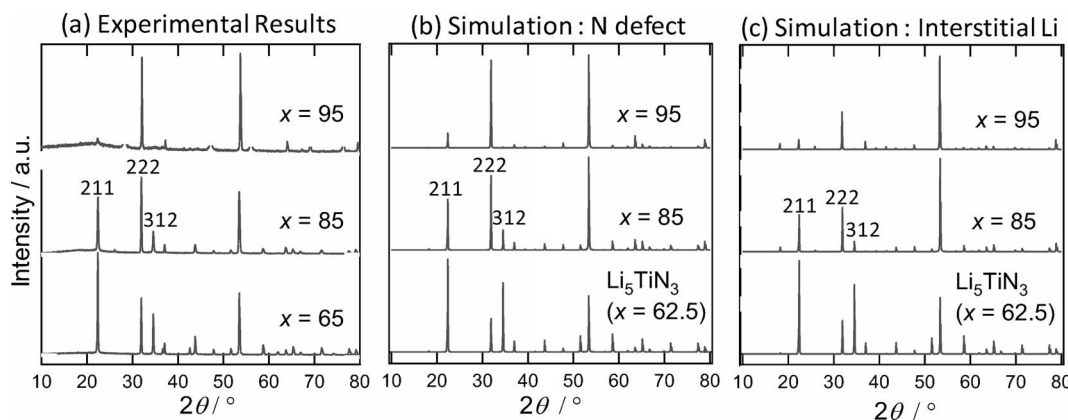


Fig. 7. X-ray diffraction patterns of the samples prepared by heating the starting mixtures with various ratios of $x\text{Li}_3\text{N}-(100-x)\text{TiN}$ ($x = 65, 85$ and 95) at 800°C in Ar (a), compared with the patterns simulated based on the nitrogen defect model of $[\text{Li}_5][\text{Li}_y\text{Ti}_{1-y}][\text{N}_{3-y}]$ (b) and the interstitial lithium model of $[\text{Li}_5][\text{Li}_{3y}][\text{Li}_y\text{Ti}_{1-y}][\text{N}_3]$ (c).

charge compensation with respect to the present preliminary analysis, more detailed investigations using neutron diffraction data would be necessary to determine the valid structure including the position and occupancy of light elements such as lithium and nitrogen.

4. Conclusion

The new lithium-rich compounds with anti-fluorite-type structure framework were synthesized in Li-Ti-N ternary system by sintering mixture of Li_3N and TiN with various ratios at 800°C under pure Ar flow. The definitive valid structure is not clear at the moment, but the preliminary analysis led to speculate the nitrogen defect model, $[\text{Li}_5]_{48c}[\text{Li}_y\text{Ti}_{1-y}]_{16c}[\text{N}_{3-y}]_{8a,24d}$.

Acknowledgement This work was financially supported by the Ministry of Education, Culture, Sports, Science and Technology of Japan, through a Grant-in-Aid for Scientific Research No. 19655074.

References

- 1) M. Nishijima, N. Tadokoro, Y. Takeda, N. Imanishi and O. Yamamoto, *J. Electrochem. Soc.*, **141**, 2996 (1994).
- 2) M. Nishijima, Y. Takeda, N. Imanishi, O. Yamamoto and M. Takano, *J. Solid State Chem.*, **113**, 205 (1994).
- 3) J. L. C. Rowsell, V. Pralong and L. F. Nazar, *J. Am. Chem. Soc.*, **123**, 8598 (2001).
- 4) M. Nishijima, T. Kagohashi, Y. Takeda, N. Imanishi and O. Yamamoto, *J. Power Sources*, **68**, 510 (1997).
- 5) A. Rabenau, *Solid State Ionics*, **6**, 277 (1982).
- 6) T. Asai, K. Nishida and S. Kawai, *Mat. Res. Bull.*, **19**, 1377 (1984).
- 7) V. W. Sachse and R. Juza, *Z. Angew. Chem.*, **278** (1949).
- 8) H. Yamane, S. Kikkawa, H. Horiguchi and M. Koizumi, *J. Solid State Chem.*, **65**, 6 (1986).
- 9) H. Yamane, S. Kikkawa and M. Koizumi, *J. Solid State Chem.*, **71**, 1 (1987).
- 10) H. Yamane, S. Kikkawa and M. Koizumi, *J. Solid State Ionics*, **15**, 51 (1985).
- 11) R. Juza and F. Hund, *J. Solid State Chem.*, **13**, 257 (1948).
- 12) H. Yamane, S. Kikkawa and M. Koizumi, *J. Solid State Ionics*, **25**, 183 (1987).
- 13) R. Juza, H. H. Weber and E. Meyer-Simon, *Z. Anorg. Allg. Chem.*, **48**, 273 (1953).
- 14) P. Chen, Z. Xiong, J. Luo, J. Lin and K. L. Tan, *Nature (London)*, **420**, 302 (2002).
- 15) R. Juza, H. H. Weber and E. Meyer-Simon, *Z. Anorg. Allg. Chem.*, **273**, 48 (1948).
- 16) R. Niewa, D. Zhrebtssov and Z. Hu, *Inorg. Chem.*, **42**, 2538 (2003).
- 17) A. Gudat, S. Haag, R. Kniep and A. Rabenau, *Z. Naturforsch. B*, **456**, 111 (1990).
- 18) R. Juza, E. Anschutz and H. Puff, *Angew. Chem.*, **71**, 161 (1959).
- 19) A. Gudat, R. Kniep and A. Rabenau, *J. Less common Metals*, **161**, 31 (1990).
- 20) T. Shodai, S. Okada, S. Tobishima and J. Yamaki, *J. Solid State Ionics*, **86-88**, 785 (1996).
- 21) D. H. Gregory, P. M. O'Meara, A. G. Gordon, J. P. Hodges, S. Short and J. D. Jorgensen, *Chem. Mater.*, **14**, 2063 (2002).
- 22) H. Yamane et al., unpublished.
- 23) F. Farges, G. E. Brown, A. Navrotsky, H. Gan and J. R. Rehr, *Geochim. Cosmochim. Acta*, **60**, 3055 (1996).
- 24) F. Farges, G. E. Brown and J. J. Rehr, *Phys. Rev. B*, **56**, 1809 (1997).